DOI: 10.1002/adma.200702753

Interfacing Functionalized Carbon Nanohorns with Primary Phagocytic Cells**

By *Stéphanie Lacotte, Ainara García, Marion Décossas, Wafa' T. Al-Jamal, Shouping Li, Kostas Kostarelos, Sylviane Muller, Maurizio Prato,* Hélène Dumortier,** and *Alberto Bianco**

Carbon nanohorns (CNHs) are a new type of single-walled carbon nanotubes (SWNTs).[1] They are composed of tubes with a diameter between 2 to 5 nm aggregated in a spherical form that resembles that of a sea urchin or a dahlia. Endowed with this unique morphology, functionalized CNHs (*f*-CNHs) are currently under careful scrutiny as novel drug containers for a controlled and timed delivery.[2–10] A prerequisite for biomedical applications is the solubility of such material. The problem of CNH solubility has been partially solved as a certain number of organic reactions can be applied to functionalize them, which makes their manipulation easier and improves their biocompatibility.[10–13] *f*-CNHs have been proposed for controlled drug release of anti-inflammatory and anticancer agents including dexamethasone, cis-platin, and doxorubicin.[3–8] Alternatively, CNHs have been modified with magnetite and administered in vivo for magnetic resonance imaging (MRI) applications.[9] These studies have been complemented by the assessment of a reduced toxicity displayed by the functionalized horns. Indeed, Isobe et al. have shown that *f*-CNHs are rapidly internalized into fibroblastic cell lines without affecting the cell viability in comparison to other inorganic nanoparticles such as quartz and TiO_2.[10] This feature renders *f*-CNHs worthy of consideration for various therapeutic applications. Another advantage in developing carbon nanohorns for biomedical applications is the complete absence of metal catalysts, necessary to produce SWNTs.[14] This is particularly important in the context of biomedical applications, because it has been demonstrated that iron particles are responsible for some degree of toxicity associated with inhaled nanotubes.[15] The incorporation of carbon-based nanoparticles in living systems is raising much concern because these types of nanomaterials could accumulate into the cells, organs, and tissues with dangerous effects.[16] In a previous study we have reported effect of functionalized SWNTs on primary immune cells.[17] Within these cell populations, macrophages play a key role in the ''surveillance'' of the body by the immune system, being responsible of the recognition and capture of the external substances and objects for their elimination. Therefore, it is of paramount importance to study the impact of novel nanomaterials such as CNHs on this type of phagocytic cells. Information on the impact of carbon-based materials on the immune system is still very limited and controversial.[18] On the basis of the available data, it is not possible to anticipate the responses resulting from the interaction of new classes of nanoparticles such as *f*-CNHs with the different cellular systems. In this study, we have explored in detail the biocompatibility of *f*-CNHs towards primary murine macrophages. The CNHs have been initially functionalized by direct addition of amine functions to render them dispersible in aqueous buffers, and subsequently labeled with a fluorescent dye for imaging. The capacity of macrophages to engulf the *f*-CNHs has been assessed by confocal and transmission electron microscopy (TEM). The impact of both cationic and fluorescently labeled *f*-CNTs on murine primary phagocytic cells was analyzed in terms of uptake, cytotoxicity, and cell activation.

The covalent functionalization of CNHs is one of the powerful approaches to improve their solubility in organic solvents and water. This allows not only the study of *f*-CNH properties in solution, but also permits to extend their

[*] Prof. M. Prato, A. García
Dipartimento di Scienze Farmaceutiche, Università di Trieste
Trieste 34127 (Italy)
E-mail: prato@units.it
Dr. H. Dumortier, Dr. A. Bianco, S. Lacotte, Dr. M. Décossas
Dr. S. Li, Dr. S. Muller
CNRS, Institut de Biologie Moléculaire et Cellulaire
UPR 9021 Immunologie et Chimie Thérapeutiques
67000 Strasbourg (France)
E-mail: h.dumortier@ibmc.u-strasbg.fr;
a.bianco@ibmc.u-strasbg.fr
Prof. K. Kostarelos, W. T. Al-Jamal
Nanomedicine Laboratory
Centre for Drug Delivery Research
The School of Pharmacy, University of London
London (UK)

[**] S.L. and A.G. contributed equally to this work. This work was supported by the ''Centre National de la Recherche Scientifique'' and the French ''Agence Nationale de la Recherche'' (grant ANR-05-JCJC-0031-01), the University of Trieste, Italian MUR (PRIN 2006, prot.2006034372 and FIRB RBIN04HC3S), Regione Friuli Venezia–Giulia, Basque Government (ETORTEK NANOMATERIALES) and the Spanish ''Ministerio de Educacion y Ciencia'' (Grant No. CSD2006-53). This work was also supported by the European Union, NEURONANO program (NMP4-CT-2006-031847). AFM and FTIR data were recorded at INASMET (San Sebastian, Spain). TEM and confocal images were recorded at the Microscopy Facility Plate-form of Esplanade Campus (Strasbourg, France). We are also grateful to Stéphane Campidelli for fruitful discussion, Jérôme Mutterer for his help on confocal microscopy measurements, and Michael Pepka, Nanocraft Inc., for a generous gift of p-CNH. Supporting Information is available online from Wiley InterScience or from the authors.

ADVANCED MATERIALS

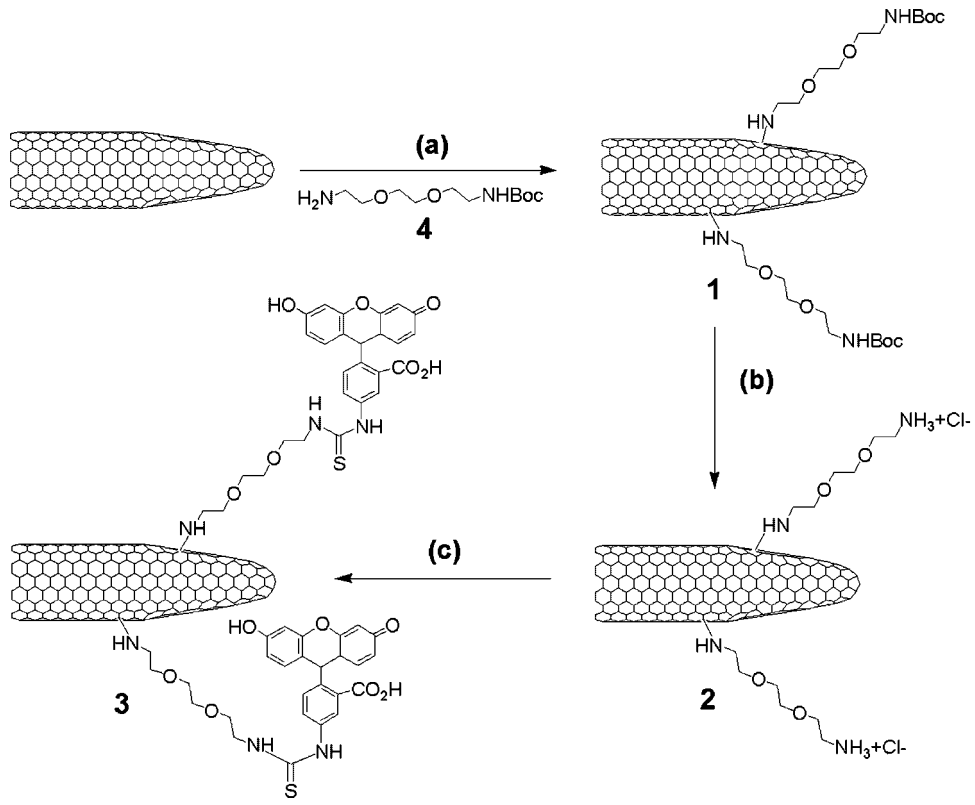

Scheme 1. Reagents and conditions: a) DMF, 50 °C, 5 days; b) gaseous HCl in DMF, room temperature (RT), 1 h; c) DMF, triethylamine, fluorescein isothiocyanate (FITC), RT, 12 h.

applications in different domains of materials science and biomedicine. One method to modify CNHs is the direct addition of amines.[10,12] The preparation of *f*-CNHs **1**–**3** is described in Scheme 1. Pristine CNHs were reacted with the Boc-monoprotected 2,2′-(ethylenedioxy)diethylamine (**4**) in *N*,*N*-dimethyl formamide (DMF), affording **1**.[12] After deprotection of the Boc group in acid conditions, the free amino groups of *f*-CNH **2** were coupled with fluorescein isothiocyanate (FITC) to obtain the labeled *f*-CNH **3**, for the cell uptake study. The excess of FITC was carefully removed by repeated washings/re-precipitations of *f*-CNH. The different *f*-CNHs were characterized by using different microscopic and spectroscopic techniques (TEM, atomic force microscopy (AFM), thermogravimetric analysis (TGA), photon correlation spectroscopy (PCS), and Fourier transform (FT)IR spectroscopy).

The amount of functional groups in the *f*-CNHs was determined by TGA. *f*-CNH **1** and **3** present a loss of weight of 2% and 4% at 500 °C, respectively (see Supporting Information, Fig. S1). This corresponds to the presence of one functional group per every 1000 C atoms of *f*-CNH **1**, giving about 80 μmol of functional groups per gram. On the other hand, *f*-CNH **3** has one functional group every 1100 C, corresponding to approximately 70 μmol of FITC per gram. The FTIR spectrum of *f*-CNH **3** (see Supporting Information, Fig. S2) confirmed the presence of the CH_2 stretching vibration bands at 2924–2856 cm^{-1}, the carbonyl stretching vibration band at 1724 cm^{-1}, the ether C–O–C stretching band at 1098 cm^{-1}, the amide I stretching band and amide II deformation band at 1664 cm^{-1} and 1580 cm^{-1}, respectively, and the amide III stretching band at 1260 cm^{-1}. Moreover, the characteristic isothiocyanate N=C=S asymmetric stretching band of the initial FITC has disappeared owing to the bond between this group and the ammonium terminal group of **2**. The amount of ammonium groups on *f*-CNH **2** was determined by a Kaiser quantitative test.[19] We found a loading of amines of 57 μmol g^{-1}. After the coupling to FITC, the Kaiser test demonstrated that 66% of the amines were functionalized, while one third remained unreacted probably because of their hampered accessibility by the fluorescent molecule. The Kaiser test values are in good agreement with those obtained with the TGA analysis. The *f*-CNHs **1**–**3** were then analyzed by TEM. The images show the presence of different *f*-CNH aggregates with a spherical morphology and of some isolated horns pointing out of the aggregates (Fig. 1A and B). The high magnification revealed the conical end caps protruding from the central core (see also Fig. S3). No structural differences were observed between *f*-CNH **1** (Fig. 1A) and **2** (Fig. 1B). The main morphological difference was observed for ammonium-terminal *f*-CNHs **2**, which were more agglomerated than the precursor *f*-CNHs **1**. In addition to TEM analysis, *f*-CNHs **3** were characterized by AFM (Fig. 1C). The AFM images displayed individual *f*-CNHs and clusters. The analysis of 19 objects allowed calculating a diameter distribution with an

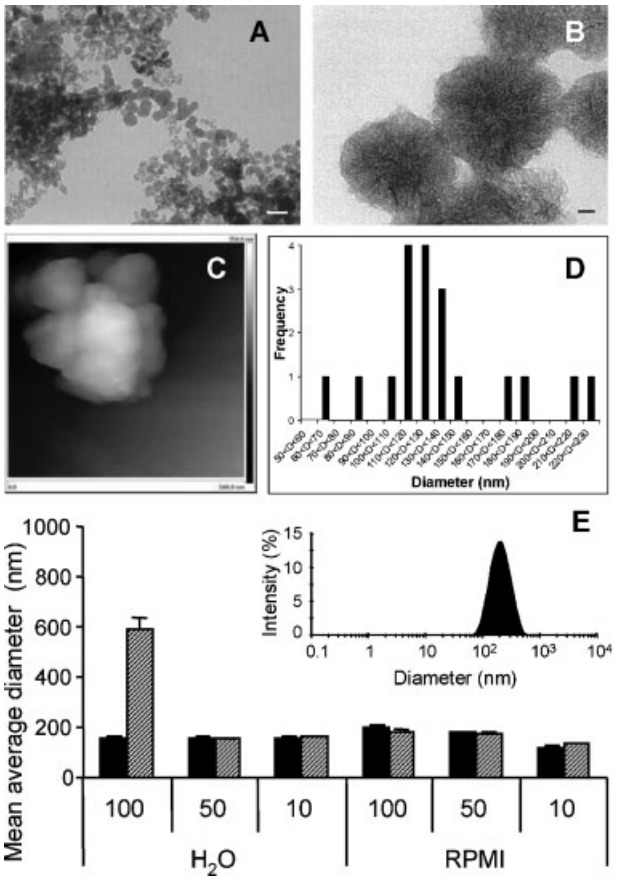

Figure 1. TEM images of A) *f*-CNH **1**, and B) *f*-CNH **2**. The nanohorns were dispersed in DMF. C) AFM image of *f*-CNH **3**, and D) diameter distribution of this sample. E) Hydrodynamic diameter of *f*-CNH **3** dispersions. Mean average diameter of different concentrations (100, 50, 10 μg mL^{-1}) of *f*-CNH **3** dispersed in H_2O and RPMI medium supplemented with 10% fetal calf serum, measured immediately after the preparation (black bar) or after 24 h (hatched bar). Mean ± standard deviation; $n = 3$. Inset: size distribution intensity of 50 μg mL^{-1} *f*-CNH **3** in RPMI immediately after preparation. Scale bars: A: 100 nm; B: 10 nm; C: *x*-axis is 500 nm.

average in the range between 110 and 130 nm (Fig. 1D). The hydrodynamic diameter of these nanometer sized particles was measured in solution using PCS. Both *f*-CNHs **2** and **3** were dispersed in water and cell culture medium (vide infra) at different concentrations. The mean average hydrodynamic diameter of *f*-CNH **3** is reported in Figure 1E (see also Fig. S5) and was within a 100–200 nm range. The values at the lowest concentration correlate nicely with the AFM measurements. The size of *f*-CNH dispersions in both H_2O and the RPMI medium was stable over 24 h, which was particularly advantageous for the subsequent cell uptake studies. However, aggregation occurred at the highest concentration in water after 24 h, probably owing to hydrophobic interactions between the *f*-CNH clusters.

Macrophages constitute the first line of defense against pathogens. They very efficiently detect and capture every intruder in the body, which triggers a cascade of events leading to inflammation. In order to investigate whether macrophages are able to sense and internalize *f*-CNHs, FITC-labeled *f*-CNHs **3** were incubated with primary peritoneal mouse macrophages for different periods of time (1–24 h). We used *f*-CNHs **3** at a concentration of 10 μg mL^{-1}, which was previously shown to be optimal in other cell penetration experiments using carbon nanotubes.[17] Similarly to functionalized SWNT,[17] the macrophages already internalized *f*-CNH **3** upon 1 h of incubation (data not shown), but the best results in terms of number of stained cells and fluorescence intensity were obtained when macrophages were cultured with *f*-CNHs **3** for a longer period of time. After 24 h incubation, most of the macrophages have uptaken *f*-CNH **3**. Moreover, *f*-CNHs **3** seem localized in the cytoplasm but not in the nucleus as no overlap with the nuclear marker DAPI (4′,6-diamidino-2-phenylindole) was observed (see Supporting Information, Fig. S6).

To more precisely analyze the distribution of *f*-CNHs in macrophages at the ultra-structural level, we then performed TEM experiments. First, the structure of *f*-CNHs **2** and **3** dissolved in water (50 μg mL^{-1}) and deposited on TEM grids was analyzed to check that they were not altered in a physiological environment. The images (Fig. 2A and B) revealed that the horns display a spherical morphology in aqueous solution and were mainly observed as small aggregates very similar to those dissolved in DMF (Fig. 1A and B). As shown in Figure 2C–E (black arrows), the same structural aspect was also observed for *f*-CNHs **3** that have been uptaken by macrophages. Moreover, *f*-CNHs **3** were found inside vesicles that correspond to macrophage-specific endocytosis vesicles called phagosomes. The horns could be also observed at the cell surface, surrounded by an invagination of the plasma membrane (Fig. 2E). All together, these observations support the idea that *f*-CNHs enter into macrophages via an endocytosis pathway. To further confirm that the structures visualized in macrophages are internalized nanohorns, we used an anti-FITC antibody conjugated to gold nanoparticles in order to detect the FITC-labeled *f*-CNHs **3**. Indeed, as displayed in Figure 2F, some gold nanoparticles, enhanced with silver, could be observed associated to spherical *f*-CNHs into the phagosomes. Unexpectedly, using this pre-embedding method for TEM analysis, we have evidenced a non-specific reaction of the horns with the silver-based enhancement reagent. We could observe large deposits of silver (1 μm or more in diameter) on *f*-CNHs **3** inside the phagosomes. To further examine this undesired reaction we deposited *f*-CNHs **2** on a TEM grid and treated them directly with the silver enhancement kit. Despite the absence of the gold nanoparticles, big clusters of metal were found associated to the horns. We believe that the high capacity of adsorption of CNHs and the defects present at their surface induce a local deposition of silver atoms that nucleates the formation of the big aggregates. In view of these results, a certain attention should be paid when carbon nanomaterials are observed using TEM and gold-labeled antibody recognition, as non-specific interactions might occur. A possible alternative to avoid these

ADVANCED MATERIALS

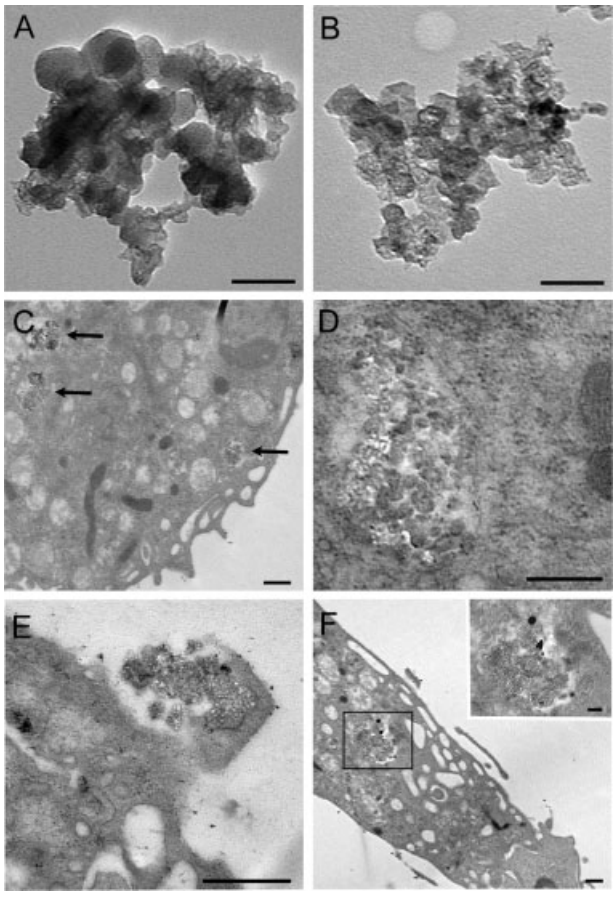

Figure 2. TEM images of *f*-CNHs. A,B) *f*-CNH **3** and *f*-CNH **2**, respectively, both dissolved in water (50 μg mL^{-1}). Images (C–E) show *f*-CNH **3** (indicated by black arrows) localized inside macrophages after 24 h incubation. *f*-CNHs **3** were also specifically detected using an anti-FITC antibody coupled to colloidal gold particles as shown in F. Inset: magnification of the surrounded area showing antibody-labeled *f*-CNHs **3**. Scale bars: A, B, D, and inset in F: 100 nm; C, E, and F: 500 nm.

side reactions is a pre-incubation of the horns with 10% bovine serum albumin (BSA), which almost completely hampers the formation of silver deposits (data not shown).

There are conflicting data on the effects of carbon-based nanomaterials on cells, some describing high toxicity and others low toxicity.[20,21] Recent publications have reported some hypotheses to explain the risk of cytotoxicity, such as the use of surfactants for solubilization[22] or the presence of metallic contaminants,[15] which is not a concern in the case of CNHs since they are synthesized without any metal catalyst.[1] In general, most contributors to the field agree that the presence and density of chemically active functional groups and the size of the particles are also two key factors in the induction of cytotoxic effects.[23] To date, only two groups have reported preliminary and rather succinct data suggesting that CNH do not exert toxic effects on cancer/transformed cell lines (ST2 bone-marrow stromal cells, MC3T3-E1 osteoblasts, 3T3 fibroblasts, and HeLa epithelial cells).[3,10] Here, we present for the first time results obtained with primary cells. *f*-CNHs were homogeneously dispersed in an aqueous solution without adding surfactants, while cell viability was evaluated using propidium iodide. Knowing that macrophages survive well in vitro for a few days without any stimulation, we examined the cell viability after 48 and 72 h of incubation with 10 μg mL^{-1} of *f*-CNHs **2** or **3**. No specific cell death could be measured in the presence of the nanohorns as compared to untreated cells (see Supporting Information, Fig. S7). This result clearly demonstrates that, even if they penetrate into cells, *f*-CNHs do not exert lethal effects (at least within a 3-day period). This is very encouraging considering a potential biomedical application of *f*-CNHs as carriers for biologically active molecules.

Macrophages are professional scavengers and very sensitive cells regarding activation and uptake, these two mechanisms being directly linked to each other. Depending on the nature of the ingested particles, the macrophage-induced immune response can be pro-inflammatory or anti-inflammatory. When the macrophages engulf self-components, such as apoptotic cells, an anti-inflammatory process starts in order to avoid autoimmune phenomena.[24] On the contrary, when they detect and capture potentially harmful elements, such as bacteria or infected cells, the macrophages activate a pro-inflammatory process in order to eliminate them.[25] Production of reactive oxygen species (ROS) is one of the key pathways involved in this process and occurs upon uptake of foreign bodies. This oxidative burst is considered as a prototype marker of macrophage activation. Therefore, we decided to measure the production of ROS in response to *f*-CNHs, using dihydroethidium which is oxidized to the fluorescent ethidium in the presence of ROS and then becomes detectable by flow cytometry. First, we checked the production of ROS in the presence of phorbol myristate acetate (PMA), which is a known strong activator of macrophages. As shown in Figure 3A and C (black curve), a peak of oxidative burst is detected very rapidly, that is, after 30 min of incubation with PMA. Then, the amount of intracellular ROS returns to the background level. A similar kinetics was previously described in response to bacteria.[25] Interestingly, macrophages incubated with 10 μg mL^{-1} of *f*-CNH **2** or **3** also produce ROS (Fig. 3B and C (bars)). However, in contrast to what was observed with PMA, the oxidative burst initiates only after 1 h of incubation with the nanohorns and persists even after 24 h of incubation. It should be noted that not only the kinetics are different upon incubation with PMA or *f*-CNHs, but also the percentage of ROS-producing cells. More than 85% of the cells were ethidium-stained when activated with PMA whereas a maximum of 60% of them produced ROS when incubated with *f*-CNHs for 24 h. This latter data supports the observations from confocal microscopy, which show that *f*-CNHs were not detected in all the cells after 24 h of incubation. In this field, contradictory results have been obtained with other carbon nanomaterials including carbon nanotubes (CNTs). One study has reported an oxidative burst in the rat macrophage cell line NR8383 in dependence on contaminants of pristine CNTs,[21] while another has described a non-significant production of ROS by the mouse RAW 264.7 cell line incubated with purified or

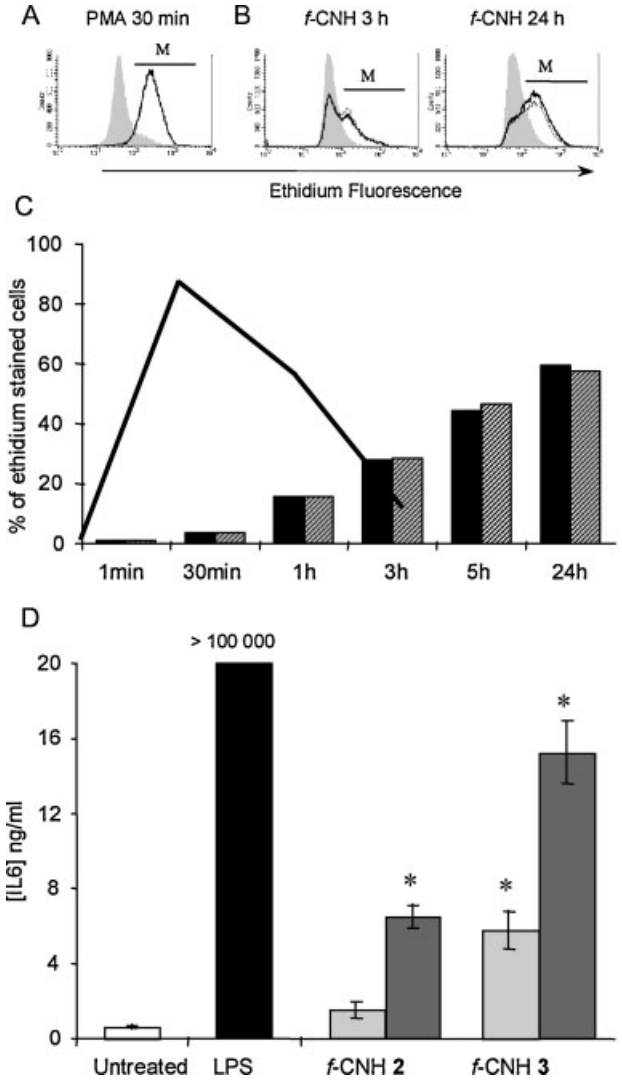

Figure 3. Macrophage activation triggered by *f*-CNHs: A–C) Measurement of the oxidative burst, and D) secretion of the pro-inflammatory cytokine IL6. A,B) Flow cytometry histograms showing cell-associated ethidium fluorescence in untreated macrophages (gray areas) or in macrophages incubated with A) PMA (0.625 μg mL^{-1}) as a positive control (dark line), or B) with 10 μg mL^{-1} of *f*-CNH **2** (shaded lines) or *f*-CNH **3** (dark lines). C) Kinetics of ROS production in macrophages in response to PMA (black curve) or *f*-CNH **2** (black bars) or *f*-CNH **3** (hatched bars). Ethidium-stained cells (expressed as % of total cells) correspond to the fluorescent cell population defined by the M region as shown in the histograms in (A) and (B). Data are derived from one representative experiment out of three. D) The cells were left untreated (white bar) or incubated with *f*-CNH **2** or **3** at 10 μg mL^{-1} (light gray bar) or at 50 μg mL^{-1} (dark gray bar). Supernatants were harvested 24 h later and IL6 concentration was assessed by ELISA. LPS (10 μg mL^{-1}; black bar) was used as a positive control of macrophage activation. Results shown consist in the mean concentrations of secreted IL6 (± s.e.m.) out of two experiments. Statistical significance is indicated by *, $p < 0.01$ (compared to untreated cells).

non-purified CNTs.[26] However, it should be mentioned that, in the latter paper, the authors performed ROS measurements in the presence of CNTs for only a short incubation time (30 min). The data we obtained demonstrate the need of a rather long contact of macrophages with *f*-CNHs to trigger an oxidative burst and to detect the production of ROS.

An oxidative stress can lead to the translocation of transcription factors to the nucleus, which in turn regulate the secretion of pro-inflammatory cytokines such as IL6.[27] In order to assess this macrophage activation parameter, cells were cultured in the presence of 10 μg mL^{-1} or 50 μg mL^{-1} of *f*-CNHs **2** or **3**. After 24 h, the supernatants were collected and assessed for their IL6 content using an enzyme-linked immunosorbent assay (ELISA) test. Alternatively, cells were stimulated with lipopolysaccharides (LPS) as a positive control. Macrophages produced significant, although moderate, amounts of IL6 when they were incubated with *f*-CNHs **2** and **3** at 10 μg mL^{-1} (1.4 ng mL^{-1} and 5.8 ng mL^{-1} of IL6, respectively) and even more in response 50 μg mL^{-1} of *f*-CNHs (Fig. 3D). These amounts are three orders of magnitude lower than those produced in response to LPS stimulation, and are in the same range as those we had previously measured in response to SWNTs functionalized using the cut/oxidation method.[17]

In summary, the organic functionalization of CNHs has permitted to render such material soluble in physiological conditions. We have obtained the *f*-CNHs by a direct addition to pristine CNHs of a diamine moiety that can be further modified with a fluorescent probe. The resulting *f*-CNHs were biocompatible and were evaluated on their capacity to be integrated into a cellular system. We have shown that *f*-CNHs are effectively phagocytozed by primary murine macrophages without affecting cell survival. However, some signs of activation, which could lead to an inflammatory status in vivo, are visible, such as a clear oxidative burst and IL6 production. The rapid uptake of this type of carbon nanoparticles can be particularly advantageous if a strategy targeting macrophages is envisaged. Many studies developing nanomaterials for biomedical and pharmaceutical applications are addressing their interactions with macrophages.[28] Indeed, these cells are the primary immune defense of the body against pathogens. They are involved in the induction of a cascade of inflammatory events and in the activation of other immune cell types, which will all play a role in the eradication of the microorganisms. The delivery of biologically active agents using *f*-CNHs, which internalize into cells and promote contemporarily the activation of the immune system, is a very promising concept.[29] Indeed, it could be interestingly exploited in a vaccination approach against infectious or cancer diseases. *f*-CNHs would simultaneously play the role of antigen carrier and adjuvant, as it has been recently proposed for other nanoparticles.[30,31] Therefore, *f*-CNHs could emerge as a novel and alternative tool for any biomedical application requiring some activation of the immune system.

Experimental

Pristine CNHs used in this work were obtained from Nanocraft, Inc. Experimental details on their functionalization to generate *f*-CNHs **2** and **3**, the characterization of the structures and morphology of these

ADVANCED MATERIALS

f-CNHs (using TEM, AFM, TGA, PCS, and FTIR), and the complete description of the experiments on the uptake, cell viability and cell activation of macrophages are reported in the Supporting Information.

Received: November 6, 2007
Published online:

[1] S. Iijima, M. Yudasaka, R. Yamada, S. Bandow, K. Suenaga, F. Kokai, K. Takahashi, *Chem. Phys. Lett.* **1999**, *309*, 165.
[2] K. Shiba, *J. Drug Targeting* **2006**, *14*, 512.
[3] T. Murakami, K. Ajima, J. Miyawaki, M. Yudasaka, S. Iijima, K. Shiba, *Mol. Pharm.* **2004**, *1*, 399.
[4] K. Ajima, M. Yudasaka, T. Murakami, A. Maigne, K. Shiba, S. Iijima, *Mol. Pharm.* **2005**, *2*, 475.
[5] T. Murakami, J. Fan, M. Yudasaka, S. Iijima, K. Shiba, *Mol. Pharm.* **2006**, *3*, 407.
[6] K. Ajima, A. Maigne, M. Yudasaka, S. Iijima, *J. Phys. Chem. B* **2006**, *110*, 19097.
[7] M. Yudasaka, J. Fan, J. Miyawaki, S. Iijima, *J. Phys. Chem. B* **2005**, *109*, 8909.
[8] K. Ajima, M. Yudasaka, A. Maigne, J. Miyawaki, S. Iijima, *J. Phys. Chem. B* **2006**, *110*, 5773.
[9] J. Miyawaki, M. Yudasaka, H. Imai, H. Yorimitsu, H. Isobe, E. Nakamura, S. Iijima, *Adv. Mater.* **2006**, *18*, 1010.
[10] H. Isobe, T. Tanaka, R. Maeda, E. Noiri, N. Solin, M. Yudasaka, S. Iijima, E. Nakamura, *Angew. Chem. Int. Ed.* **2006**, *45*, 6676.
[11] N. Tagmatarchis, A. Maigne, M. Yudasaka, S. Iijima, *Small* **2006**, *2*, 490.
[12] C. Cioffi, S. Campidelli, C. Sooambar, M. Marcaccio, G. Marcolongo, M. Meneghetti, D. Paolucci, F. Paolucci, C. Ehli, G. M. Rahman, V. Sgobba, D. M. Guldi, M. Prato, *J. Am. Chem. Soc.* **2007**, *129*, 3938.
[13] C. Cioffi, S. Campidelli, F. G. Brunetti, M. Meneghetti, M. Prato, *Chem. Commun.* **2006**, *2129*.
[14] D. Tasis, N. Tagmatarchis, A. Bianco, M. Prato, *Chem. Rev.* **2006**, *106*, 1105.
[15] A. A. Shvedova, E. R. Kisin, A. R. Murray, V. Z. Gandelsman, A. D. Maynard, P. A. Baron, V. Castranova, *J. Toxicol. Environ. Health Part A* **2003**, *66*, 1909.
[16] V. L. Colvin, *Nat. Biotechnol.* **2003**, *21*, 1166.
[17] H. Dumortier, S. Lacotte, G. Pastorin, R. Marega, W. Wu, D. Bonifazi, J.-P. Briand, M. Prato, S. Muller, A. Bianco, *Nano Lett.* **2006**, *6*, 1522.
[18] L. Lacerda, A. Bianco, M. Prato, K. Kostarelos, *Adv. Drug Delivery Rev.* **2006**, *58*, 1460.
[19] V. Georgakilas, N. Tagmatarchis, D. Pantarotto, A. Bianco, J.-P. Briand, M. Prato, *Chem. Commun.* **2002**, *3050*.
[20] L. Ding, J. Stilwell, T. Zhang, O. Elboudwarej, H. Jiang, J. P. Selegue, P. A. Cooke, J. W. Gray, F. F. Chen, *Nano Lett.* **2005**, *5*, 2448.
[21] K. Pulskamp, S. Diabaté, H. F. Krug, *Toxicol. Lett.* **2007**, *168*, 58.
[22] N. A. Monteiro-Riviere, A. O. Inman, Y. Y. Wang, R. J. Nemanich, *Nanomedicine* **2005**, *1*, 293.
[23] C. M. Sayes, F. Liang, J. L. Hudson, J. Mendez, W. Guo, J. M. Beach, V. C. Moore, C. D. Doyle, J. L. West, W. E. Billups, K. D. Ausman, V. L. Colvin, *Toxicol. Lett.* **2006**, *161, 135*.
[24] A. M. Johann, A. von Knethen, D. Lindemann, B. Brüne, *Cell Death Differ.* **2006**, *13*, 1533.
[25] S. Perticarari, G. Presani, E. Banfi, *J. Immunol. Methods* **1994**, *170*, 117.
[26] V. E. Kagan, Y. Y. Tyurina, V. A. Tyurin, N. V. Konduru, A. I. Potapovich, A. N. Osipov, E. R. Kisin, D. Schwegler-Berry, R. Mercer, V. Castranova, A. A. Shvedova, *Toxicol. Lett.* **2006**, *165*, 88.
[27] V. Castranova, *Free Radical Biol. Med.* **2004**, *37*, 916.
[28] F. Chellat, Y. Merhi, A. Moreau, L. Yahia, *Biomaterials* **2005**, *26*, 7260.
[29] J. M. Shaw, W. S. Futch, L. B. Schook, *Proc. Natl. Acad. Sci. USA* **1988**, *85*, 6112.
[30] T. Uto, X. Wang, K. Sato, M. Haraguchi, T. Akagi, M. Akashi, M. Baba, *J. Immunol.* **2007**, *178*, 2979.
[31] H. Hasegawa, T. Ichinohe, P. Strong, I. Watanabe, S. Ito, S. Tamura, H. Takahashi, H. Sawa, J. Chiba, T. Kurata, T. Sata, *J. Med. Virol.* **2005**, *75*, 130.

